Monitoring VHE Extragalactic sources with the ARGO-YBJ detector

M. ZHA[1] ON BEHALF OF ARGO-YBJ COLLABORATION
[1]*Institute of High Energy Physics*
zham@ihep.ac.cn

Abstract: Detecting and monitoring emission from flaring gamma ray source in the Very-High-Energy (VHE, $>$100 GeV) band is a very important topic in the gamma ray astronomy. The ARGO-YBJ experiment, featured with high duty cycle and wide field of view, is particularly capable of detecting flares from extragalactic objects. On the basis of a fast reconstruction and analysis, a real time monitoring to selected VHE extragalactic sources is implemented.

Keywords: monitoring, flaring phenomenon, VHE extragalactic source, ARGO-YBJ

1 Introduction

Up to date more than 40 extragalactic sources with energy above 100 GeV have been detected by IACTs. Most of these sources, around 30, belong to a blazar class of AGNs with a common feature of BL Lac objects. The emission from blazars is highly variable and characterized by a flaring behavior, in which the flux increases dramatically on various time scales, even down to the hour time scale. For example in May 1994, the Whipple telescope observed a significant variability within few hour timescale for the TeV gamma-rays from Mkn421. In this period the average source flux above 250 GeV has increased by a factor of 10 [1]. Many interesting works can be done with flaring phenomenon or variability studies. For instance spectral variations of gamma-rays from the sources are treated as a useful tool to understand the physics of the source. Therefore study or monitor their variability with sufficiently low exposure times is necessary.

High duty cycle ($\sim$95%) and wide aperture ($\sim$2 sr) of ARGO-YBJ allow the detection of flaring behavior associated with these AGN, especially during daytime transits. Two very interesting flare events have been observed by the experiment: one is that in June 2008 when ARGO-YBJ successfully observed the Mkn421 flaring event on a timescale of 3 days whereas IACT could not due to moonlight[2]; another is that in Feb. 2010 ARGO-YBJ caught an excess signal around 4 s.d. from Mkn421 within a one-day transit[3], which is the first time for ground-based experiment to reach this level within one day. Above observations confirm that ARGO-YBJ enables the real-time monitoring the transient phenomenon associated with variable sources.

A list of VHE extragalactic candidates collected by R. Wagner[4] were chosen for the monitoring procedure. From this list, only 31 sources were within the field of view of the ARGO-YBJ detector. (zenith $< 40^\circ$) In addition, VHE L3+C [6] was added to the list upon the authors' interest. And Crab nebula was added to supervise frequently the monitoring procedure and ensured that it operates in a stable manner.

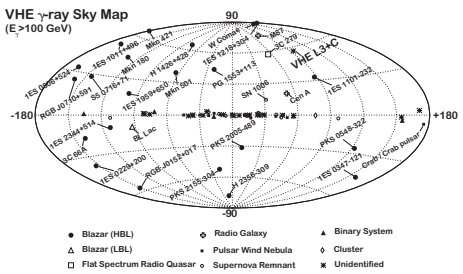

Figure 1: The skymap containing all the selected sources.

2 ARGO-YBJ experiment

The ARGO-YBJ experiment is located at the Yang-Ba-Jing Cosmic Ray Observatory (Tibet, P.R.China, 30.11°N, 90.53°E) at an altitude of 4300 m a.s.l., corresponding to a vertical atmospheric depth of $606\ \mathrm{g/cm^2}$. It consists of a single layer of Resistive Plate Chambers with each RPC ($285 \times 122.5\ \mathrm{cm^2}$) divided into 10 basic detection units called PADS ($55.6 \times 61.8\ \mathrm{cm^2}$). Each PAD consists of 8 digital readout strips. 12 RPCs are grouped into a cluster ($5.7 \times 7.6\ \mathrm{m^2}$). The central carpet ($78 \times 74\ \mathrm{m^2}$) of the detector is fully covered by 130 clusters, 23 additional clusters form a guard ring surrounding the central carpet extending the total area to $11,000\ \mathrm{m^2}$. In order to extend the dynamic range, a charge read-out layer has been implemented by installing each RPC with two Big Pads [5]

Two independent DAQ system are implemented in the detector: the scale mode and the shower mode. In this work, just the data from shower mode is used. In shower mode, the arrival time and location of each fired pad are recorded for later geometry reconstruction. The trigger threshold is the number of fired pads higher than 20 within 420 ns triggering window, and the trigger rate is about 3.5 kHz. The ARGO-YBJ has been taking data with its full layout since November 2007.

3 Monitoring Scheme

3.1 Time calibration, event selection and reconstruction

In this fast reconstruction mode, time calibration data for the last period is used instead of those of current period, which will be officially produced every 10 days based on the data. Figure 2 shows the distribution of the opening angle using different time calibrations for the same sets of data. The difference is less than 0.1° which should bring marginal effect while considering that the angular resolution of the detector is about 0.8° at the hit multiplicity great than 100.

A single run of ARGO-YBJ detector usually lasts about a couple of hours, whose raw data are split into tens of files, each with duration about 7 minutes. A raw data file is transferred to IHEP and INFN computer center by internet soon after its creation, usually within half an hour. After receiving a file, a reconstruction program starts automatically to process it. Considering the high trigger rate of the detector and the limited angular resolution at low energy, only events with the number of fired pads greater than 100 can be used, which imposes that the median value of the energy distribution is 1.8 TeV. On a typical CPU a file can be reconstructed within 2 hours and in average 15 CPUs are employed daily.

3.2 search for excess

The surrounding region method is used for estimating the background. The details about this method can be found in [6]. And the Li-Ma prescription[7] was adopted to calculate the significance. Because of the source does not reside exactly at the center of a sky cell due to the pre-defined divisions of the sky cell yet without optimization to any source, 36 shifts had been employed on every sky cells, with a space of 1/6 cell width both in declination and right ascension. Among these shifts only 24 nearest sky cells were adopted, which confined the maximum distance between center of sky cells and the source to 0.86°. These 24 sky cells are overlapped and correlated, only the maximum significant excess among these cells are kept, indicating the significance of the source.

Up to date, no well accepted models have been developed to understand the duration of the transient flaring phenomemon, the observation facts of Mkn421 indicating that

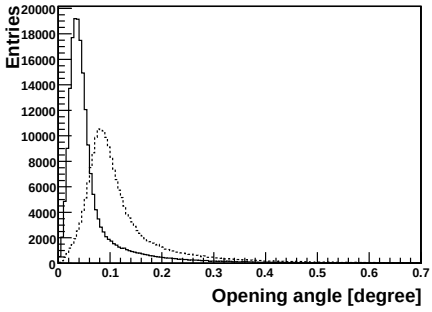

Figure 2: Distribution of the space angle between two directions of an event reconstructed based on two different time calibration data. The solid line represents two consecutive time calibration data, whereas the dashed line is for two time calibration data separated by 30 days.

a flare may last from several hours to several days. Thus in this analysis, each source are monitored until it disappeared from the field of view of the detector (zenith $> 65^\circ$). Upon its disappearance, the excess significances of 1, 2, 4, 8 transits (i.e., sidereal days) were calculated immediately, and the maximum was taken to indicate the significance of the source of that day.

3.3 Alarm settings

From above sections it is known that the excess of any source was searched from nearby 24 sky cells and in 4 time binnings, and the significance was evaluated once per sidereal day. Severe correlations exist in both space and time, no simple distribution can be used to calculate the chance probability of an excess. In this case, a Monte Carlo simulation which emulates the search procedure for a single source was made to sort out the significance distribution, assuming that there were no signal emissions from the source. Figure 3 gives the simulation result, whose mean is 1.814 and RMS is 0.705, the number of events is corresponding to number of days. Apparently it is not a Gaussian distribution. Further simulation results, green line in Figure 3, confirm the fact that the distribution does not depend on the background intensity in the sky cell.

From this plot, the chance probability for a significance threshold can be obtained. After converting the chance probability to time duration, the relationship between number of years for a single source or 33 sources and the significance threshold can be obtained, as show in figure 4, from which it is seen that thresholds of 4.30 s.d. and 5.02 s.d. are corresponding to once per 5 years for a single source and 33 sources respectively.

These 33 sources were classified into two categories based on the observation history: (i) sources with flares intensive

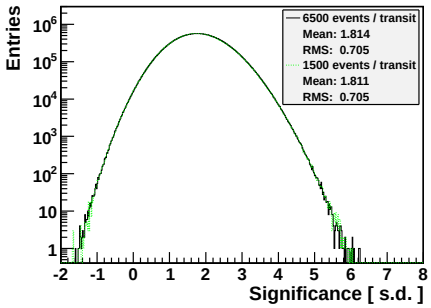

Figure 3: Distribution of significances obtained from a MC simulation. The black and green line background intensity is 6500 and 1500 respectively

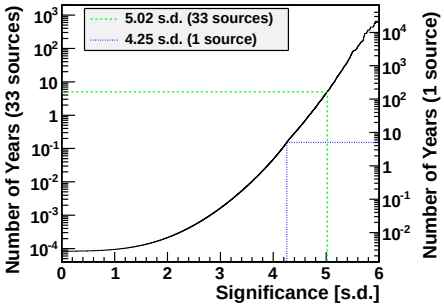

Figure 4: Number of years for 1 occurrence versus the significance threshold. The left y-axis is corresponding to 33 sources, and the right one is for a single source.

enough which have been observed, such as Mkn421, and (ii) other sources whose flares have not been detected yet. The threshold for sources in the first category is set to 4.30 s.d., and that for the other is 5.02 s.d. Once a source is detected to exceed its significance threshold, an alarm e-mail would be immediately and automatically sent to people concerned. If a source in category (ii) is detected above its threshold, it would be manually elevated to category (i). This guarantees that the source could be monitored in a more active state hereafter, and any subsequent flares can be notified more timingly.

In addition to the occasional alarm e-mail, daily reports summarizing excess information of all the sources for the past day would be sent to a few people concerned. This monitors the running status of the whole analysis procedure.

4 Results and the frequency analysis

4.1 Testing of the scheme with historic data

A re-discovery of observed results is a good indication to verify the whole analysis scheme. The data from Jan. to July in the year of 2008 was used when Mrk 421 was in

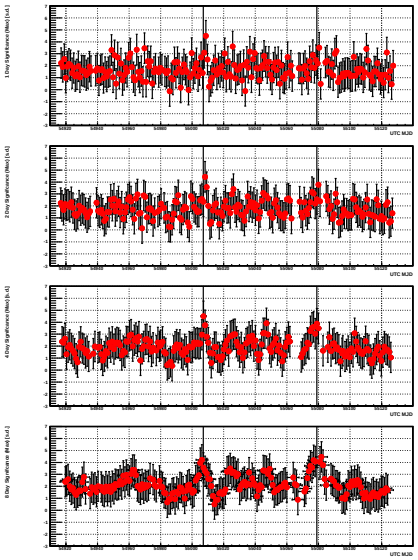

Figure 5: Monitoring history of Mrk 421: the rolling significance of the excess found around the Mrk421 for 1, 2, 4, 8-day time scales

active status. Fig.5 shows the rolling significance around Mkn421 for 1, 2, 4, 8 days. Under the existed alarming threshold, two flares, April 2008 and June 2008 detected by ARGO-YBJ were re-discovered and alarmed in 1-, 8-day transits. This proves the validity of the whole analysis scheme. In Fig.5 the significances and their errors are represented respectively by red dots and black error bars. The vertical black line represents the flaring events from SWIFT, which were also observed by the ARGO-YBJ experiment. For reason of clarity only exclusive data points were drawn with solid markers.

4.2 Frequency study on excesses of a source

Since July 2010, the monitor has started to process the new data, however nothing have been found until now. Limited by the sensitivity of the detector, some flares of a frequent flaring source may have shown some excesses but unfortunately not detected with enough significances. As a supplement, high frequency of occurrence of significant excesses may indicate an unusual state of a source. For instance, not any excess from Mkn421 above the threshold 5.02 s.d. (of category ii) in the past 3 years, but 4 excesses have ever occurred above 4.30 s.d. (of category i), much higher than the number of expected occurrences 0.6 (= 3 years / 5 years). Even if its flares had not been detected and confirmed by other analyses, it would still deserve attentions from us.

The monitoring results of the whole 3 years are explored further more for less significant flares. As for the frequency study, correlations of observations make things very complex. For example, an excess lasting for 8 days may show up in several consequent days with high significances. Such kind of correlation effects must be eliminated as far as possible for a reliable analysis. For this purpose,

a selection to significant excesses have been imposed additionally: for a particular source in any consecutive 8 days, at most 1 excess above 4.30 s.d. can be held - if there are more, keeping only the biggest one. This selection criteria has been applied to both the data and the simulation.

Excesses of a source above 4.30 s.d. is sorted from big to small, marked with $i = 1, 2, 3, \ldots$. the chance occurrence $Q_{\rm i}$ (defined as the expected number of occurrences of an event due to background fluctuations, which was firstly introduced in [6]) of excess i is calculated based on the simulated probability $P_{\rm i}$ and total number of transits $N_{\rm transit}$ in the 3 years,

$$Q_{\rm i} = P_{\rm i} \times N_{\rm transit}. \quad (1)$$

The Poisson probability $P_{\rm i}^{\rm poisson}$ of the number of excesses $\geq i$ is then obtained,

$$P_{\rm i}^{\rm poisson} = \sum_{k=i}^{\infty} \frac{Q_{\rm i}^k}{k!}^{-Q_{\rm i}}. \quad (2)$$

Among these series of values, the minimum $P_{\rm min}^{\rm poisson}$ is kept to represent the chance probability of the frequency. For $N_{\rm source} = 33$ sources, the chance occurrence turns to be $Q = P_{\rm min}^{\rm poisson} N_{\rm source}$, which finally is converted to chance probability $P = 1 - {}^{-Q}$. Table 1 lists these values for all the 33 sources, and figure 6 is drawn too for a visual comparison.

Table 1: List of parameters about the frequency analysis for all the 33 sources.

Nr	$N_{\rm transit}$	$\sigma_{\rm max}$	$\mathcal{Q}_{\rm i}$	$\mathcal{P}$
0 (Mkn 421)	1165	4.500	4.866×10^{-1}	5.262×10^{-2}
1 (Mkn 501)	1154	4.567	4.223×10^{-1}	9.075×10^{-1}
2 (1ES 2344+514)	1161	4.717	8.335×10^{-2}	9.412×10^{-1}
3 (1ES 1959+650)	1165	3.890		
5 (1H 1426+428)	1162	3.777		
6 (M87)	1161	4.374	3.743×10^{-1}	1.000
8 (1ES 1218+304)	1164	4.095		
10 (1ES 1101-232)	1142	4.557	1.689×10^{-1}	9.968×10^{-1}
11 (PG 1553+113)	1146	4.638	1.177×10^{-1}	9.817×10^{-1}
12 (MKn 180)	1167	4.309	4.951×10^{-1}	1.000
14 (BL Lacertae)	1155	4.388	3.518×10^{-1}	1.000
15 (1ES 0229+200)	1157	4.927	1.664×10^{-1}	3.459×10^{-1}
16 (1ES 0347-121)	1153	4.023		
17 (1ES 1011+496)	1163	4.378	4.198×10^{-1}	2.654×10^{-1}
18 (3C 279)	1154	4.101		
19 (RGB J0152+017)	1152	4.203		
20 (1ES 0806+524)	1162	3.986		
21 (W Comae)	1163	3.992		
22 (S5 0716+71)	1166	4.344	4.267×10^{-1}	1.000
23 (3C 66A)	1164	4.519	4.222×10^{-1}	2.689×10^{-1}
26 (RGB J0710+591)	1163	4.068		
27 (PKS 1424+240)	1158	3.615		
28 (NGC 253)	1131	4.099		
29 (M82)	1162	5.035	1.811×10^{-2}	4.597×10^{-1}
30 (VER J0521+211)	1159	4.400	3.364×10^{-1}	1.000
31 (RBS 0413)	1160	4.370	3.801×10^{-1}	1.000
32 (1ES 0414+009)	1159	4.401	3.530×10^{-1}	8.215×10^{-1}
33 (1ES 0502+675)	1162	4.254		
35 (PKS 1510-089)	1143	4.771	6.411×10^{-2}	8.869×10^{-1}
36 (RGB 0648+152)	1153	4.343	4.255×10^{-1}	1.000
37 (IC 310)	1163	3.817		
38 (VHE L3+C)	1151	4.742	1.915×10^{-1}	4.252×10^{-1}
39 (Crab)	1158	4.655	1.090×10^{-1}	9.754×10^{-1}

Among all the sources, Mkn421 manifests a very small chance probability as 0.037, indicating its flaring history in the past 3 years. Other 5 sources show also low chance probabilities less than 0.5, hinting they may have flared but the further evidence is needed.

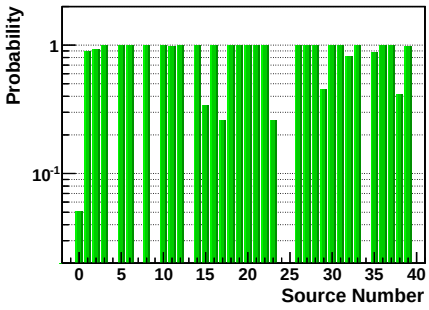

Figure 6: Chance probabilities of all the 33 sources obtained from the frequency analysis.

5 Conclusion

With the high duty cycle and wide field of view of ARGO-YBJ detector, a real-time monitoring and alerting system for selected VHE extragalactic sources has been established. A detected flare event can be notified to the community within 3 hours; A web page releasing daily monitoring report is under construction. The procedure have been successfully proved to be capable of detecting two Mkn421 flares. In addition, data in the past 3 years have been analyzed, and it shows that, except for Mkn421, no flare from other candidates has been detected. But a frequency study indicate several sources may have ever flared and more evidences are still required to make a definite conclusion.

References

[1] A.D. Kerrick *et al.*, ApJ, 438 (1995) L59.
[2] G. Aielli *et al.*, ARGO-YBJ Collaboration, APJL, 714 (2010) L208.
[3] B. Bartoli *et al.*, ARGO-YBJ Collaboration, ApJ (2011) accepted.
[4] R. Wagner, *http://www.mppmu.mpg.de/rwagner/sources/*.
[5] G. Aielli *et al.* ARGO-YBJ Collaboration, NIMA 562 (2006) 92.
[6] O. Adriani *et al.*, L3+C Collaboration, APP 33 (2010) 24.
[7] T.B. Li and Y.Q. Ma, ApJ, 272 (1983) 317.